Geo-Mar Lett
DOI 10.1007/s00367-006-0019-1

ORIGINAL

Carsten Scheuer · Karsten Gohl · Gleb Udintsev

Bottom-current control on sedimentation in the western Bellingshausen Sea, West Antarctica

Received: 27 April 2005 / Accepted: 3 April 2006

Abstract A set of single- and multi-channel seismic reflection profiles provide insights into the younger Cenozoic sedimentation history of the continental rise in the western Bellingshausen Sea, west and north of Peter I Island. This area has been strongly influenced by glacially controlled sediment supply from the continental shelf, interacting with a westward-flowing bottom current. From south to north, the seismic data show changes in the symmetry and structure of a prominent sediment depocentre. Its southernmost sector provides evidence of sediment drift whereas northwards the data show a large channel-levee complex, with a western levee oriented in the opposite direction to that of the drift in the south. This pattern indicates the northward-decreasing influence of a westward-flowing bottom contour current in the study area. Topographic data suggest the morphologic ridges at Peter I Island to be the main features responsible for variable bottom-current influence, these acting as barrier to the bottom current and entrained sedimentary material. West of Peter I Island, the east-orientated Coriolis force remains effective in deflecting the suspended load of the turbidity currents towards the west, thereby promoting growth of the western channel levee. Calculated sediment accumulation rates based on seismic data reveal Depocentre C to consist of younger Cenozoic material supplied by glacial transport and modified by contour currents in the western Bellingshausen Sea. These findings demonstrate that the shape, structure and distribution of sediment mounds and estimates of sediment accumulation rates can be associated to the influence of bottom currents and their long-term evolution in response to tectonic movements, ice-sheet dynamics and deep-water formation.

C. Scheuer (✉) · K. Gohl
Alfred Wegener Institute for Polar and Marine Research (AWI),
Postfach 120161,
27515 Bremerhaven, Germany
e-mail: cscheuer@awi-bremerhaven.de
Tel.: +49-471-48311948
Fax: +49-471-48311926

G. Udintsev
Vernadsky Institute of Geochemistry and Analytical Chemistry,
Russian Academy of Sciences,
19 Kosygin St.,
117975 Moscow, Russia

Introduction

The production of sediment along the Antarctic continental margin is primarily controlled by glacial processes, in particular since the late Miocene when the periodic development of large and thick ice masses on the West Antarctic continent resulted in high sediment supply to the continental margin. Grounding ice streams transported sedimentary material to the continental shelf and slope, and gravity-driven processes (such as slumps, slides, debris flows and turbidity currents) caused by slope failures, tectonic stress and meltwater discharge transferred slope deposits to the continental rise (e.g. Cooper et al. 1991; Bart and Anderson 1995; McGinnes et al. 1997; Anderson et al. 2001). In this way, a variety of large sediment mounds were formed on the continental rise. These mounds are widespread features in Antarctic glaciomarine depositional environments, as shown by numerous studies conducted along the West Antarctic Pacific margin (e.g. Hampton et al. 1987; Tomlinson et al. 1992; Larter and Cunningham 1993; Rebesco et al. 1996, 1997, 2002; Nitsche et al. 1997; Lucchi et al. 2002).

The development of sediment mounds is influenced by variable interactions of turbidity currents, hemipelagic sedimentation, the Coriolis force and bottom-current activity (e.g. Faugères et al. 1999; Rebesco and Stow 2001). Current measurements conducted on the continental rise of the western Antarctic Peninsula (AP; Camerlenghi et al. 1997) and in the vicinity of the South Shetland Islands (Nowlin and Zenk 1988) show evidence of a weak south-westward-flowing bottom current following the seafloor topography. Nowlin and Zenk (1988) and Camerlenghi et al. (1997) interpret this deep water mass as Weddell Sea Deep Water (WSDW) outflow through topographic gaps in the South Scotia Ridge. The bottom current is consistent with the development of sediment drifts on the western AP

continental rise since the late Miocene. Furthermore, finely laminated silty clays deposited during the so-called drift-maintenance stage and drilled during DSDP Leg 35 (sites 325 and 324, Tucholke and Houtz 1976) and ODP Leg 178 (sites 1095, 1096 and 1101, e.g. Barker and Camerlenghi 2002) can be considered as contouritic sediments.

The interaction of various transport processes is controlled by factors including the inclination of the continental slope, slope stability, sediment grain size and the strength of bottom currents. Depending on the nature of this interaction, various characteristic types of sediment mounds are produced. Channel-related contourite drifts and individual sediment mounds have been observed along the Antarctic Peninsula margin (e.g. Rebesco et al. 1997) whereas a wide trough-mouth fan has been identified along the continental margin in the central Bellingshausen Sea (Scheuer et al. 2006).

In the western Bellingshausen Sea, processes influencing sediment accumulation in the vicinity of Peter I Island are still poorly understood (Fig. 1). Satellite-derived gravity maps suggest that tectonic features of the oceanic crust may have an important effect on seafloor topography

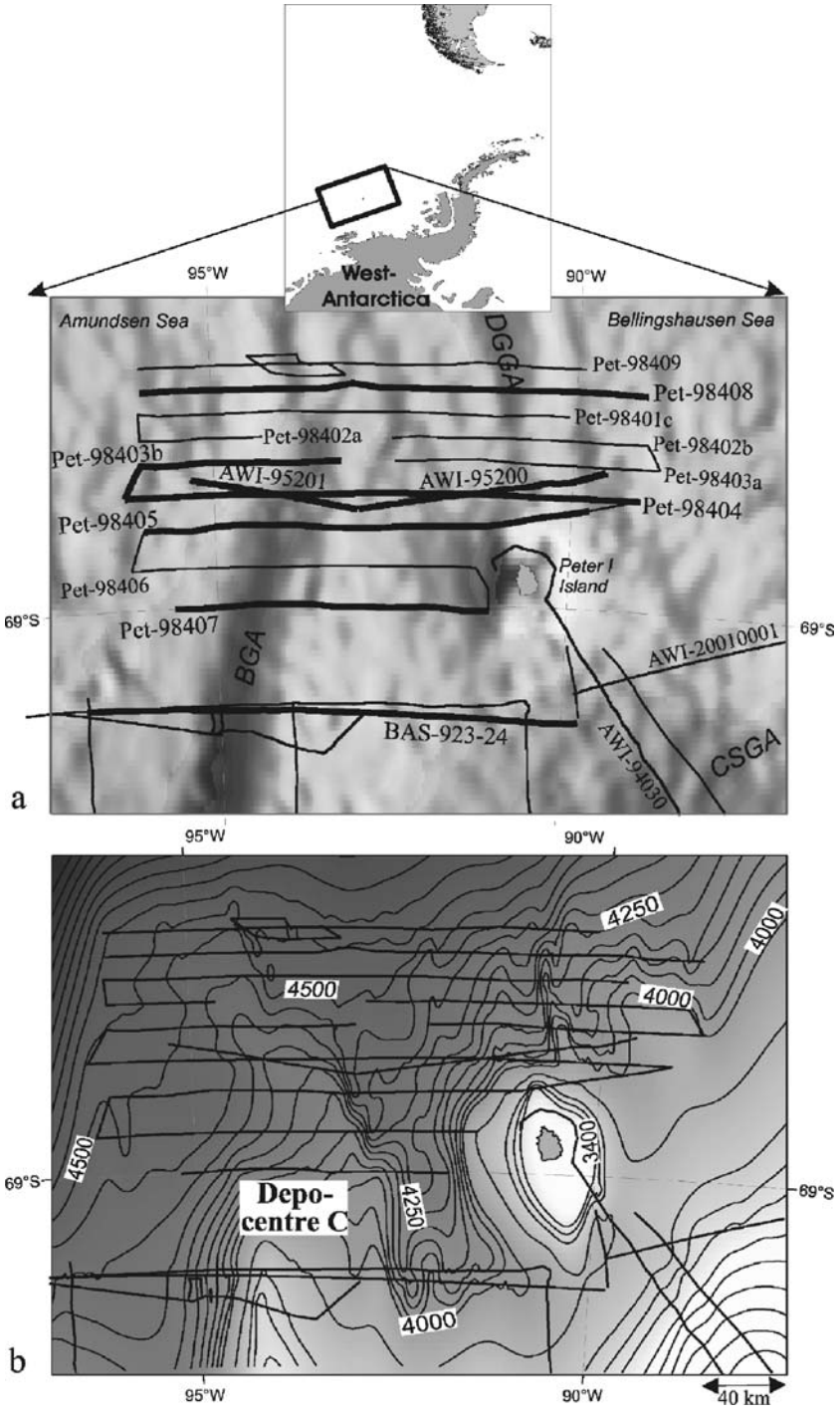

Fig. 1 **a** Track chart superimposed on a satellite-derived gravity map (Smith and Sandwell 1997) of the western Bellingshausen and eastern Amundsen Sea in the vicinity of Peter I Island. Tracks of seismic profiles selected for this study are in *bold lines*. The *thin lines* show other seismic profiles. Major gravity anomalies mark topographic and tectonic features (*BGA* Bellingshausen Gravity Anomaly, *CSGA* Continental Slope Gravity Anomaly, *DGGA* DeGerlache Gravity Anomaly). **b** Gridded bathymetric map of the study area, derived from interpolated seismic data. The *isolines* show water depths in meter

in this region. Peter I Island is a relatively young volcanic island constituting an important morphologic feature which may have shifted the path of the westward-flowing bottom current and, hence, sedimentation in this sector of the oceanic basin. In this paper, we evaluate seismic reflection data to assess the influence of morphologic and tectonic structures on sedimentation processes west and north of Peter I Island.

Study area

The study area is located in the western Bellingshausen Sea, southeast Pacific Ocean, on the West Antarctic continental rise. The region is characterized by a rough seafloor morphology caused mainly by tectonic activity, as reflected in gravity and seismic data (Fig. 1a). Two major gravity lineations, the Bellingshausen Gravity Anomaly (BGA) extending NNE from the margin to approx. 68°S, and the DeGerlache Gravity Anomaly (DGGA) extending north from Peter I Island across the DeGerlache seamounts to approx. 62°S, correspond to former plate boundaries. The BGA represents the transpressional eastern boundary of the formerly detached Bellingshausen Plate (Gohl et al. 1997; Cunningham et al. 2002; Eagles et al. 2004), which merged with the Antarctic Plate about 61 Ma bp This plate boundary is characterized by a downdipping slab, a vertical basement offset of about 7 km and an accretionary sedimentary wedge (Gohl et al. 1997; Cunningham et al. 2002). The DGGA shows a tectonic scar caused by the initiation of the Phoenix-Pacific spreading ridge at about the same time (Larter et al. 2002; Eagles et al. 2004). A set of partly exposed north-trending basement ridges underlies the DGGA (Dietmar Müller, pers. comm.).

The seafloor morphology is characterized mainly by two prominent topographic highs—Peter I Island, which forms the upper part of a northward-continuing seamount located approx. 400 km off the Eights Coast of Ellsworth Land, and an elongated, northward-dipping sedimentary depocentre in the west (Fig. 1b). Water depths above the southern crest of the depocentre are around 3,600 m, increasing to about 4,500 m in the north. The two topographic highs are separated by a south–north-orientated valley which widens towards the north. In this valley, water depths vary from 4,200 m in the south to 4,600 m in the north.

Materials and methods

The geophysical datasets used in this study were acquired during three marine expeditions (Fig. 1). The RV *Akademik Boris Petrov* expedition no. 29 in 1998 (Udintsev et al. 1999) resulted in the acquisition of more then 2,450 km of single-channel seismic (SCS) data. These comprise a set of nine parallel and sub-parallel seismic profiles (PET-98401c to PET-98409) north and west of Peter I Island, obtained using a single seismic hydrophone. Due to technical difficulties, the data were largely not available in digital form but only as paper plots. We scanned these plots and vectorised the seismic traces for digital processing. As part of the procedure, a new trace spacing was implemented with interpolated coordinates.

The multi-channel seismic (MCS) profiles AWI-95200 and AWI-95201 were acquired during the RV *Polarstern* cruise ANT-XII/4 in 1995, using an array of eight 3-l airguns and a seismic streamer with an active length of 2,400 m. Acquisition and processing of profile BAS-92324, which was acquired during a RRS *James Clark Ross* cruise in 1993, is described in Cunningham et al. (1994).

For the present study, we selected five SCS profiles from the RV *Boris Petrov* cruise and three MCS profiles from the RV *Polarstern* and RRS *James Clark Ross* cruises (Fig. 1a, bold lines). Due to the low quality and low resolution of the SCS profiles, the basement surface and the reflections associated with deep sediments can be identified only in a few locations. Reflections from younger sedimentary sequences are of better quality. The distinct and continuous reflections of the MCS profiles AWI-95200 and AWI-95201 were used to constrain the analyses of the adjacent SCS profiles PET-98404, PET-98403a and PET-98403b.

In order to convert the two-way travel time (TWT, s) data of the seismic profiles into depths (m) for subsequent estimates of sediment thicknesses and accumulation rates, we used the interval velocities obtained via processing of the MCS data. The average interval velocity of profile ANT-95201 inside the western levee (above unconformity LB, cf. below) was determined to be about 1,700 m/s. We adopted this value for estimates of thickness of sediment-drift unit E1a (cf. below) and of channel levees along the other profiles.

Results

Two characteristic types of sediment mounds were identified in the study area.

1. *Channel levees*, representing overspill deposits composed of fine suspended sediment associated with turbidity currents (Fig. 2a). These are slightly asymmetrical, the channel walls having steep slopes, the flanks shallower slopes. Along the continental margin of West Antarctica, the western levees are often higher than the eastern levees due to the Coriolis force which diverts the overspill towards the west.
2. Channel-related *sediment drifts*, characterized by a marked asymmetrical shape with a steep and a more gently sloping side (Fig. 2b). The steep side often shows faults and slope failures, whereas reflections on the shallower slope are rather plane and lie sub-parallel to parallel. In contrast to the channel levees, most of the

sediment drifts rise higher above the surrounding seafloor and are related to bottom currents which transport suspended load away from the channels. In the following, the study profiles are described from south to north.

Profile BAS-92324

Profile BAS-92324 (Fig. 3) is located closest to the continental margin. It crosses one of the largest sediment mounds (about 130 km wide and 700 m high) of the West Antarctic continental margin, referred to as Depocentre C by Scheuer et al. (2006). This mound developed on the elevated basement at the eastern side of the tectonic boundary defined by the BGA. It is characterized by a steep western and a more gently sloping eastern side, and thus resembles a sediment drift. For this profile, Cunningham et al. (2002) defined two major sedimentary units, units E1 and E2, separated by unconformity RU1 (Fig. 3). Unit E2 is subdivided into subunits E2a, E2b and E2c, associated with different stages of sedimentation prior to and during uplift (Cunningham et al. 2002; Scheuer et al. 2006). Detailed study of unit E1 indicates various stages of drift development on the gentler drift slope, which justifies the subdivision into subunits E1a and E1b proposed by Cunningham et al. (2002). Whereas unit E1b shows mainly parallel and continuous high-amplitude reflections, the reflections in unit E1a are disturbed and of weak and laterally variable amplitudes. Three recent channels have developed at the lower end of the western, gentler slope separated by sediment mounds. The middle and oldest channel, channel 2, which has a more elevated levee to the west, shows the deepest depression. The seismic reflections suggest the development of channel 2 from the base of unit E1a.

Profile PET-98407

Profile PET-98407 (Fig. 4), west of Peter I Island, is the southernmost of the SCS profiles, approx. 55 km north of profile BAS-92324. The seafloor topography is characterized by an asymmetrical channel-levee system. The deep channel at trace 700 is flanked by a small (about 0.08 s TWT) and gently westward-dipping eastern levee, and a wide and strongly elevated (about 0.3 s TWT) western levee. The western levee extends up to trace 1,750, representing an asymmetrical sediment mound with a steep eastern and a more gently sloping western side. Its east–west extension is about 140 km. The uppermost part of the western levee (0.2 s TWT) is characterized by reflections parallel to the surface. The base of this levee cannot be clearly identified due to low data quality, but the reflections below 6.0–6.1 s TWT have a different orientation, leading us to estimate the base of the levee at about 6.1 s TWT. Reflections at 6.1–6.6 s TWT reveal a depression at trace 1,000, of which the western flank ascends until trace 1,500. The inclination corresponds to that of unconformity RU1 on profile BAS-92324 (Fig. 3). Reflections of basement structures and deep sediment deposits are scarce. However, changing amplitudes on the corresponding analogue plot indicate faint basement structures below 6.8 s TWT.

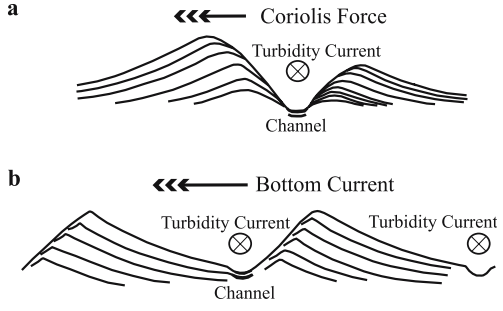

Fig. 2 **a**, **b** Schematic illustration of two potential depositional mechanisms on the continental rise, fed by the fine fraction of suspended material transported by turbidity currents (flow direction away from the observer). **a** Channel-levee deposits are controlled by the Coriolis force, or **b** deposits are formed by bottom currents, resulting in the development of sediment drifts (modified after Rebesco et al. 1996)

Profile PET-98405

The eastern part of profile PET-98405 (Fig. 5) crosses the rising northern flank of Peter I Island (Fig. 1). To the west, the profile shows the distal continuation of the asymmetrical channel-levee system seen on profile PET-98407. The elevation difference between the two levees is 0.2 s TWT. The uppermost 0.25 s TWT of the eastern levee is characterized by smooth undulating and sub-parallel reflections. The western levee slopes gently downwards towards the west up to trace 2,650. Although the base of this levee cannot be defined accurately, horizontal reflections possibly constituting base reflectors were identified at 6.3 s TWT between traces 2,300 and 2,500. At the western end of the profile (trace 3,300), a depression of the seafloor may indicate another channel.

Profiles AWI-95200 and AWI-95201

The MCS profiles AWI-95200 and AWI-95201 are oriented obliquely to the SCS profiles and to cross profile PET-98404 at common depth points (CDPs) 3,200 and 2,000, respectively (Fig. 6). The profiles cover the elevated seafloor in the east and the channel-levee system in the west. An unconformity, named LB and marking the base of the levee, extends across the entire profile at a depth of about 6.2 s TWT. On profile AWI-95200, the parallel reflections above LB dip towards the west whereas parallel- and sub-parallel-orientated reflections below LB are horizontal. On profile AWI-95201, unconformity LB can be clearly identified as the base reflector of the western channel levee, highlighted by the downlapping reflections. The unconformity constitutes the palaeo-seafloor prior to the development of the channel-levee system. Reflections below LB are horizontal and sub-parallel to parallel,

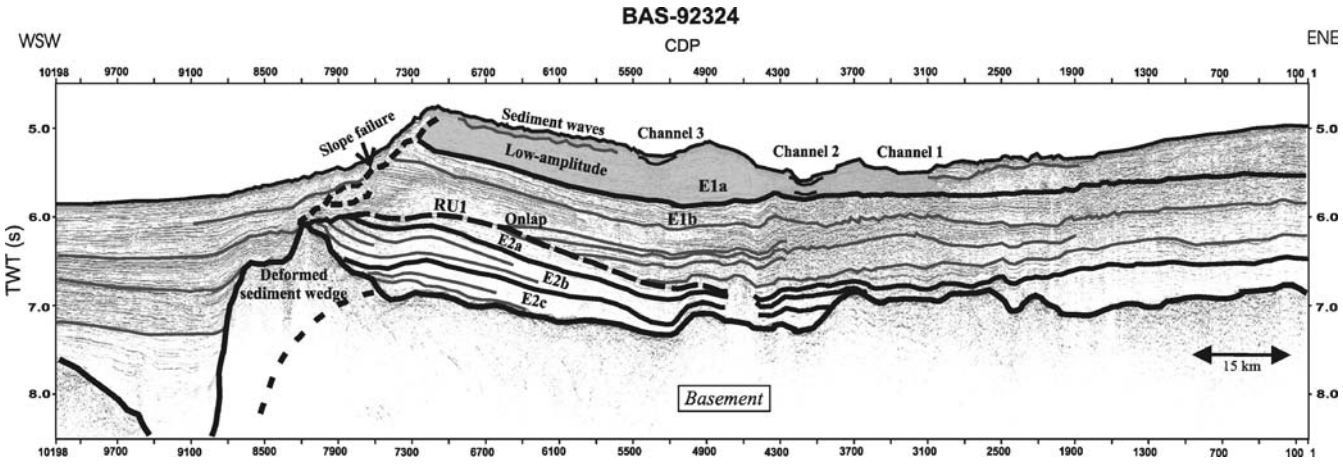

Fig. 3 MCS profile BAS-92324 with stratigraphic units modified after Nitsche et al. (1997), Cunningham et al. (2002), and Scheuer et al. (2006). Unconformity *RU1* is considered to have been caused by tectonic uplift east of the Bellingshausen Gravity Anomaly until about 61 Ma, subunits *E2a*, *E2b* and *E2c* may represent different stages of sedimentation prior to and during uplift, and changing reflection characteristics of unit E1 indicate various stages of drift development on the more gently sloping drift side, justifying a division into subunits *E1a* and *E1b* (cf. Cunningham et al. 2002; Larter et al. 2002; Scheuer et al. 2006; see text for further information)

showing variable amplitudes. The deepest sedimentary reflections of this seismic profile are observed at 7.4 s TWT below the western channel levee in a basement trough beneath the BGA (between CDP 1,500 and 2,700). The seismic data show a rough basement-sediment boundary, and subsidence of the basement west of the BGA (CDPs 2,700–3,200). Two narrow and seismically opaque domes suggest magmatic intrusions north of Peter I Island (at CDP 1,500 of AWI-95200) and west of the BGA (at CDP 3,500 of AWI-95201).

Profile PET-98404

The eastern part of profile PET-98404 (Fig. 7) shows rough seafloor north of Peter I Island, which is dissected by several gullies and channels (between traces 2,300 and 3,000). The uppermost sediments (0.3 s TWT) show smoothly undulating reflections oriented parallel to the westward-dipping seafloor to a channel at trace 1,600. The difference in elevation between the eastern and the western channel levee is 0.1 s TWT. The bulge of the western levee extends to trace 900, showing a width of about 65 km. It is characterized by parallel surface reflectors in the uppermost 0.2 s TWT. In contrast to the levee reflections, the reflections at 6.3–6.6 s TWT show a smooth depression at

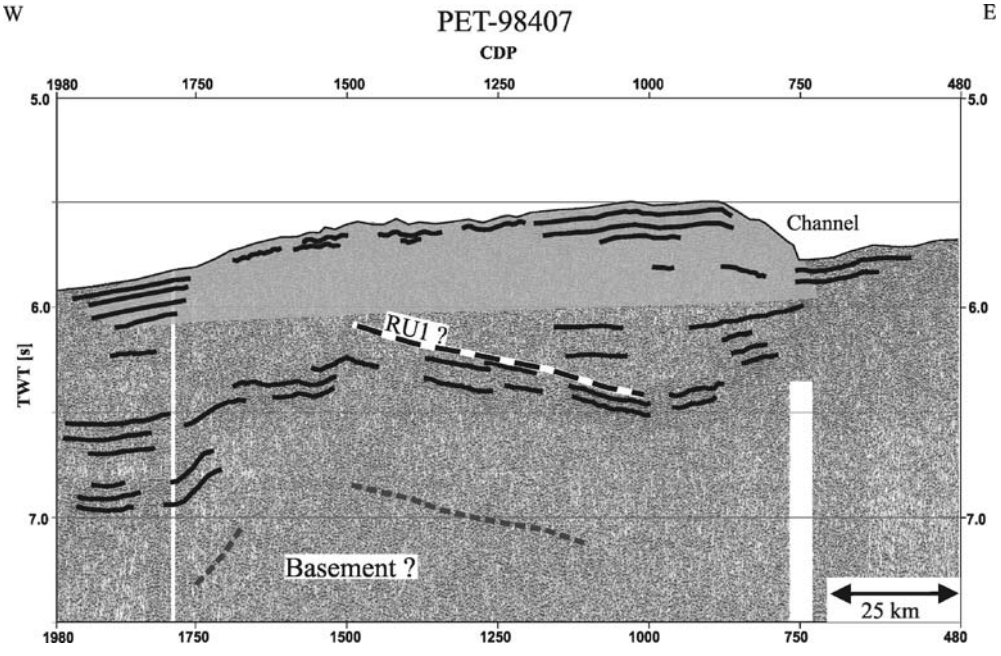

Fig. 4 SCS profile PET-98407 with *lines* indicating seismic reflections. The western channel levee is marked in *non-stippled grey*. The *black/white dashed line* denotes the unconformity *RU1* which was defined on profile BAS-92324 (Fig. 3). The *black dashed line* shows faint basement structures as identified on the original analogue plot (cf. text for more information)

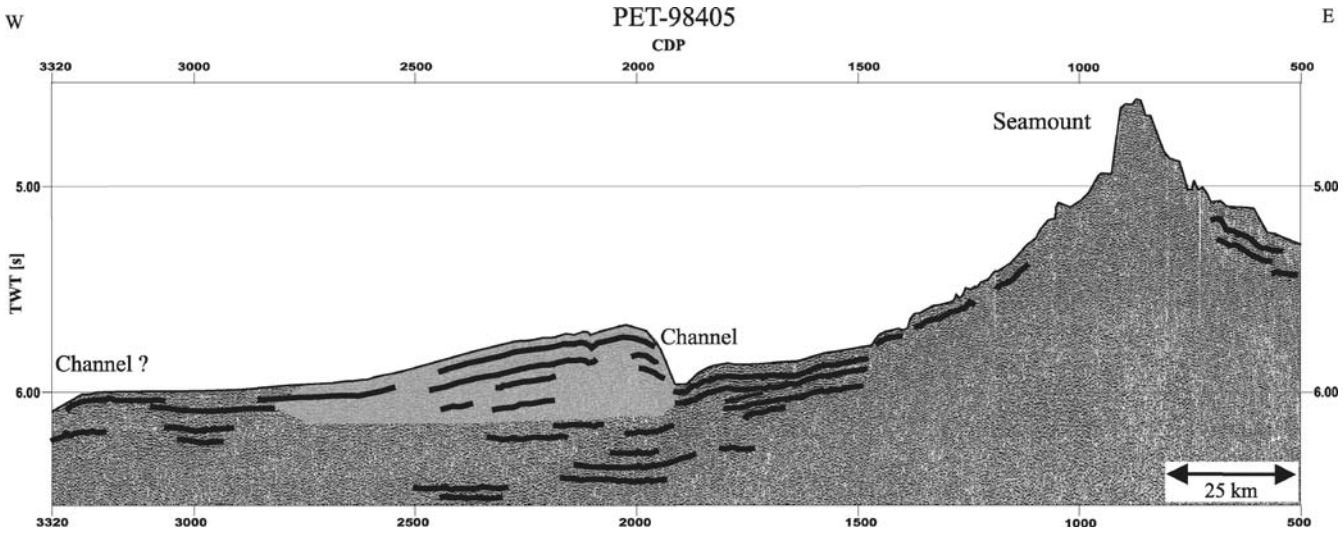

Fig. 5 SCS profile PET-98405 with *lines* indicating major seismic reflections. The western channel levee is marked in *non-stippled grey*

trace 1,250. Between traces 500 and 600, the deformed reflections below 6.3 s TWT may indicate the southern continuation of the magmatic intrusions seen on profiles AWI-95200 and AWI-95201.

Profile PET-98403b

The section of the channel-levee system shown on profile PET-98403b (Fig. 8) has a lower relief than do the profiles to the south. A prominent feature of the western levee is its subdivision into three small sediment mounds (m1, m2 and m3), which widen from east to west. The uppermost 0.1–0.2 s TWT of the western levee is characterized by smooth undulating reflectors parallel to the seafloor. The base of the western levee can be approximated by near-horizontal reflectors at about 6.2 s TWT below m1 and m2, as well as by downlapping westward-dipping reflections west of trace 1,100.

Profile PET-98408

Profile PET-98408 (Fig. 9), which represents the northernmost profile of this study, has the smoothest relief. The eastern part of the profile is characterized by high-amplitude and smoothly undulating reflections in the uppermost 0.3 s TWT. Single wave-shaped reflections can be recognised down to 6.8 s TWT. Reflections which can be interpreted as the base of the western levee appear at

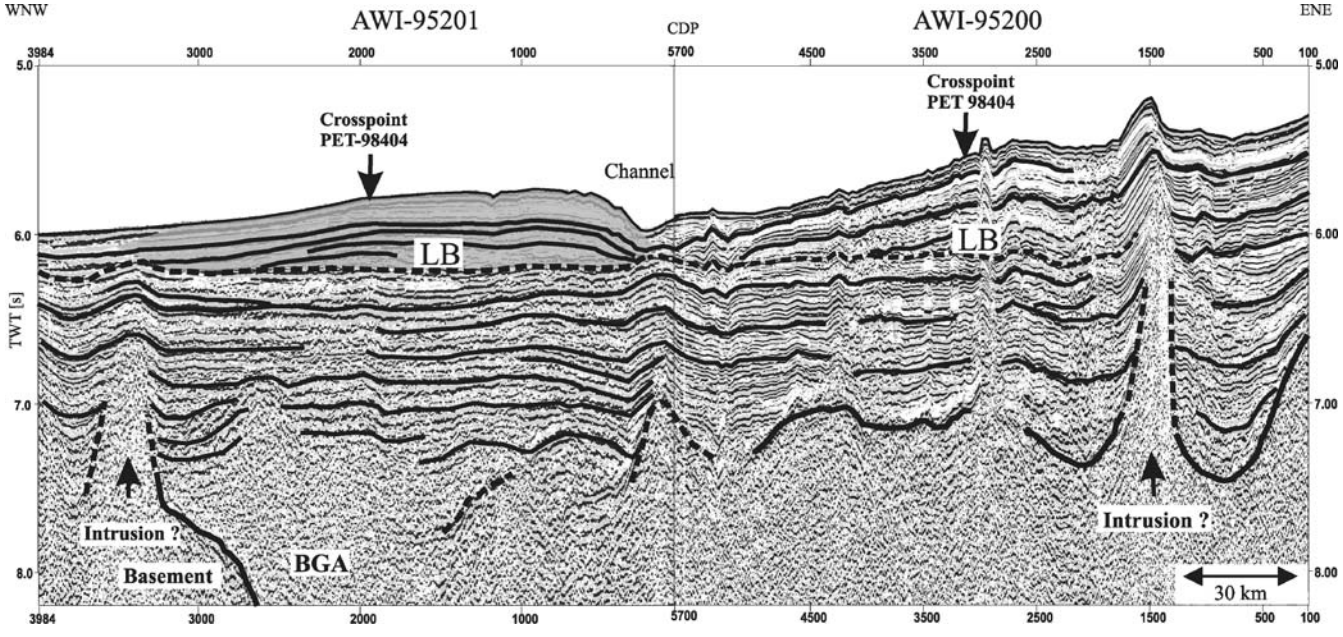

Fig. 6 MCS profiles ANT-95200 and ANT-95201 with *lines* indicating major seismic reflections. The western channel levee is marked in *non-stippled grey*. The *dashed line* represents the base of the channel levee (*LB*). *BGA* Bellingshausen Gravity Anomaly

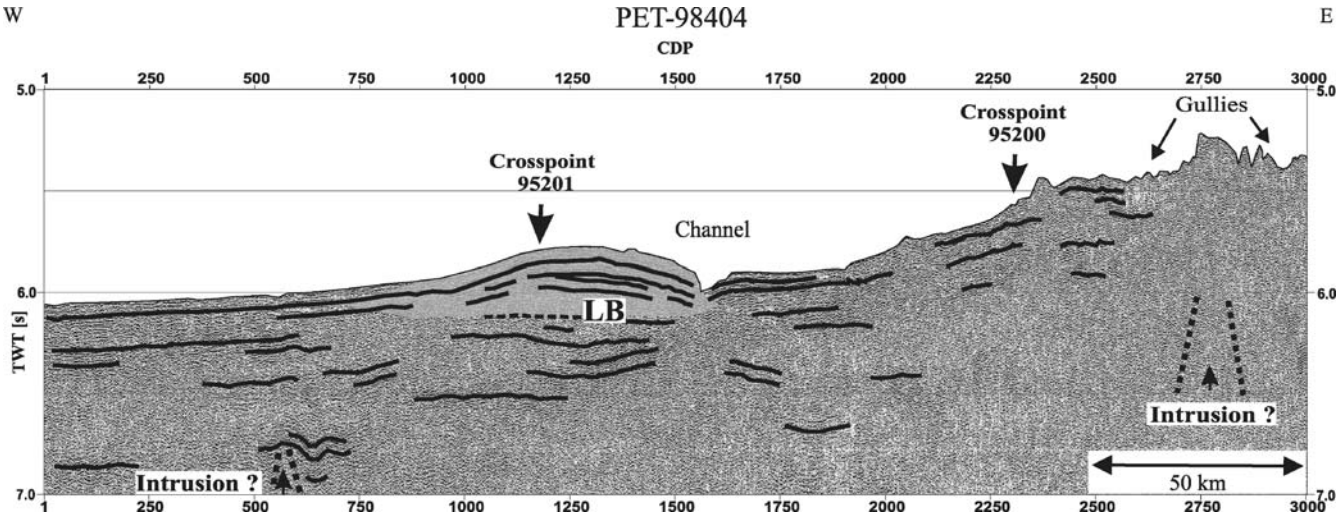

Fig. 7 SCS profile PET-98404 with *lines* indicating major seismic reflections. The western channel levee is marked in *non-stippled grey*. *LB* Base of channel levee

6.3 s TWT. To the west (at about CDP 3,500), there is a smooth depression of the seafloor. Reflections at trace 3,400 indicate a bulge at 6.6–7.0 s TWT.

Discussion and conclusions

Variations of depositional conditions

The compilation of the SCS and MCS profiles from the continental rise around Peter I Island (Fig. 10) reveals changes in depositional conditions and a topographically rough seafloor from the upper rise northwards into the deep-sea basin. The structure of the southern part of Depocentre C shows the characteristics of a sediment drift (profile BAS-92324) previously described in detail by Nitsche et al. (2000), Cunningham et al. (2002) and Scheuer et al. (2006). These characteristics are very similar to those of contourite drifts identified further east on the continental rise of the western Antarctic Peninsula, which are considered to have been developed under the influence of a bottom contour current flowing eastwards along the continental slope (e.g. Rebesco et al. 1996, 1997, 2002). The drift structure in the southern part of Depocentre C can thus be interpreted as an indicator that a bottom current affected sedimentation also in the western Bellingshausen Sea.

Rather than observing a continuation of this sediment drift structure towards the north, we documented a classical channel-levee structure approx. 55 km farther north on profile PET-98407. The wide western levee shows a short eastern flank dipping steeply into the channel and a long, more gently sloping western flank, i.e. the reverse of the pattern documented for the sediment drift in the south. In addition, slope failures observed on the steep drift side on profile BAS-92324 are not evident on profile PET-98407.

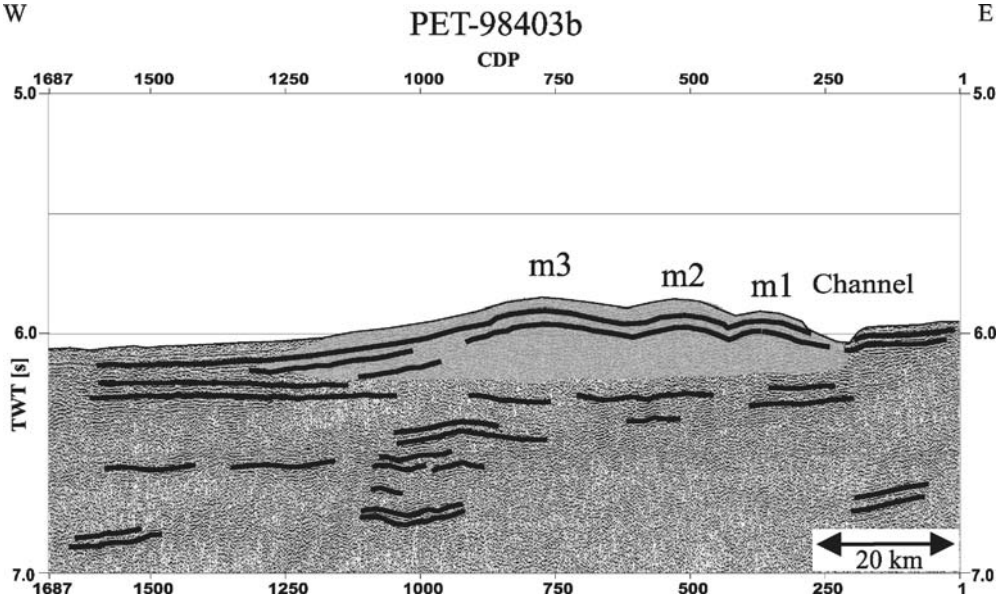

Fig. 8 SCS profile PET-98403b with *lines* indicating major seismic reflections. The western channel levee is marked in *non-stippled grey* (*m1–m3* sediment mounds)

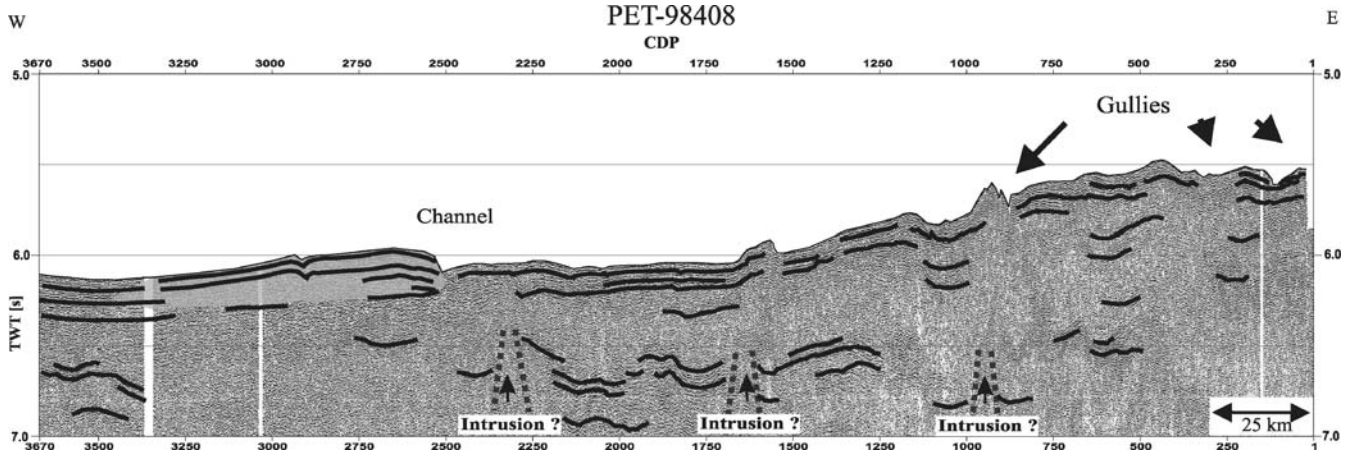

Fig. 9 SCS profile PET-98408 with *lines* indicating major seismic reflections. The western channel levee is marked in *non-stippled grey*

These findings strongly suggest a marked change in depositional conditions in the study area, implying a decreasing influence of the bottom current towards the north. Furthermore, we found no evidence of any continuation of all three channels to the north, which contrast with the observations made for profile BAS-92324. Either the three channels merge into one channel somewhere between these two profiles, or only one

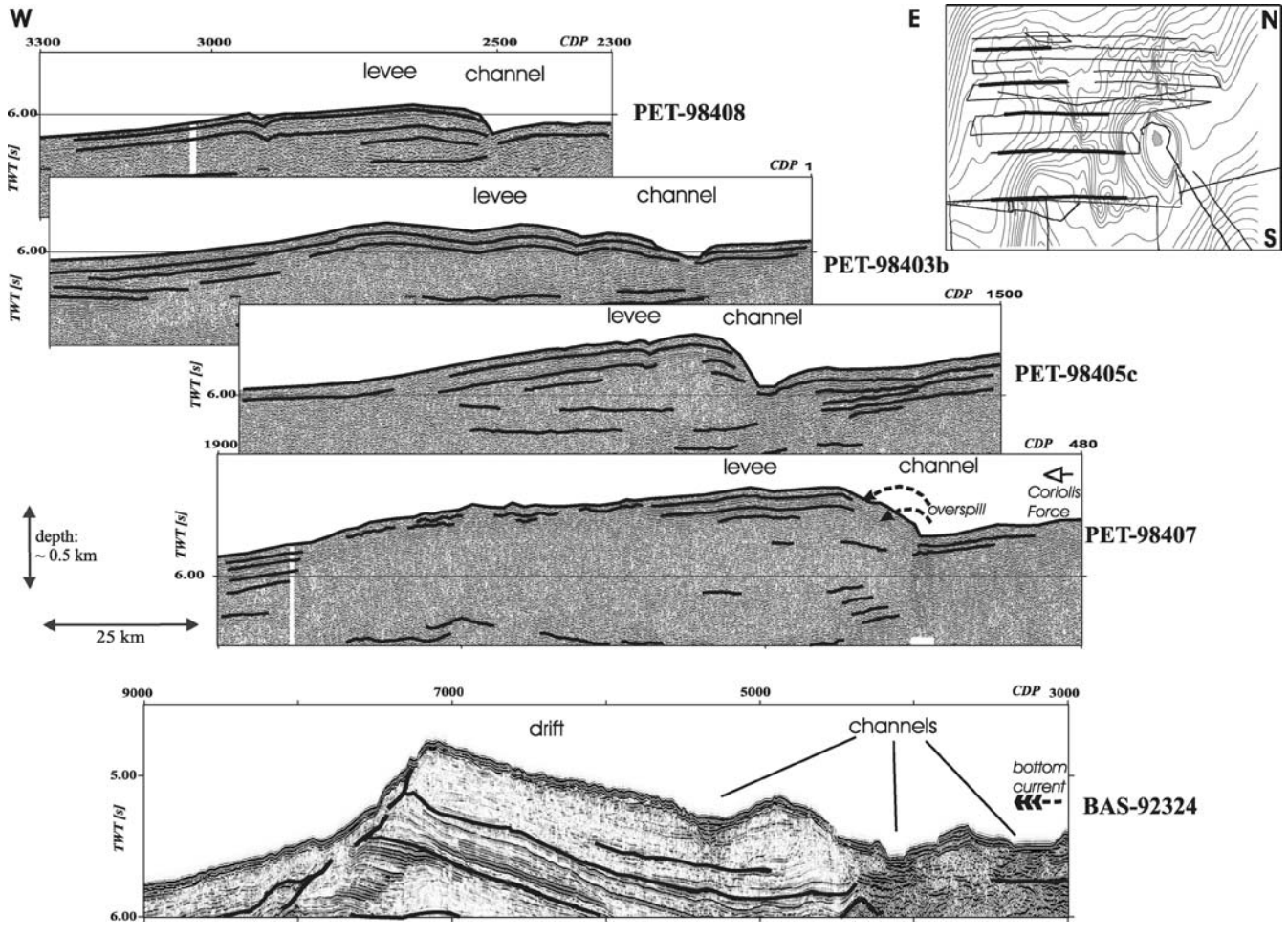

Fig. 10 Composite seismic cross-sections of Depocentre C, showing structural changes from south to north. Profile BAS-92324 is closest to the continental slope and shows a sediment drift structure with a steep side towards the west and a more gently sloping side towards the east. By contrast, the four PET profiles show a channel-levee system with the steep slope towards the east and the gentler slope towards the west

channel continues towards the deeper continental rise (Fig. 10). The higher elevation of the western levee can be explained by the influence of the Coriolis force. This causes a deflection of the suspended turbiditic sediment load towards the west, thereby enhancing sediment accumulation on the western channel side.

Exact reconstruction of the change of depositional conditions between profiles BAS-92324 and PET-98407 was not possible due to a lack of direct correlation between individual reflections. The existence of channel levees beneath channel-related sediment drifts is a relatively common feature of the Antarctic continental rise, having been reported from the western Antarctic Peninsular (Rebesco et al. 2002) and the Riiser Larsen Sea (Kuvaas et al. 2004). Contourites often appear close to the slope, associated with proximal turbidites, whereas the deeper parts of the continental rise and abyssal plains are dominated by distal turbidites. However, the observed transformation of a contourite drift into a 'simple' channel-levee system over a distance of approx. 55 km, as revealed in Depocentre C, is so far unique on the Antarctic continental margin.

Further north, the western levee becomes narrower and steeper on the eastern side (Fig. 10). Highly energetic turbidity currents flowing through the channel may be responsible for the marked steepness of its eastern flank. The narrowing of the levee may be further evidence for the decreasing influence of bottom-current flow on sedimentation. The three mounds (m1–m3) on profile PET-98403b may constitute three minor depocentres of mainly turbiditic material. Whether this can be explained by a stronger influence of bottom currents on sediment accumulation here than is the case for profile PET-98405, which is affected mainly by the Coriolis force, remains unclear. Separation into three mounds by low-energy erosional channels may be another explanation, although the seismic data do not indicate any high-amplitude reflections consistent with consolidated sediments at the base of erosional channels. In any case, this subdivision of the channel levee into a number of minor mounds is only local. The northernmost profile PET-98408 shows a weakly developed and undivided western channel levee, suggesting decreasing energy of distal turbidity currents.

The unconformity RU1 defined on profile BAS-92324 (Fig. 3) is considered to have been caused by tectonic uplift of the seafloor east of the BGA until about 61 Ma bp (Cunningham et al. 2002; Larter et al. 2002). RU1 seems to continue to the north, as indicated by the inclination of the deeper reflections on profile PET-98407 (dashed line in Fig. 4). However, reflections showing a similar inclination cannot be identified on profiles further north. We therefore infer the disappearance of this unconformity to be due to a decrease in uplift to the north. The seismic data north of Peter I Island show a decreasing roughness of the seafloor to the north. Small and narrow depressions in the western part of profile PET-98404 suggest that channels and gullies produced by erosional downslope processes become less steep to the north, as indeed seen on profiles PET-98403a and PET-98408. Furthermore, magmatic intrusions have affected sedimentation almost up to the present-day seafloor, as seen on profile ANT-95200. Unfortunately, the low quality of the SCS data does not allow us to better constrain the influence of intrusions and other basement structures on these sediments.

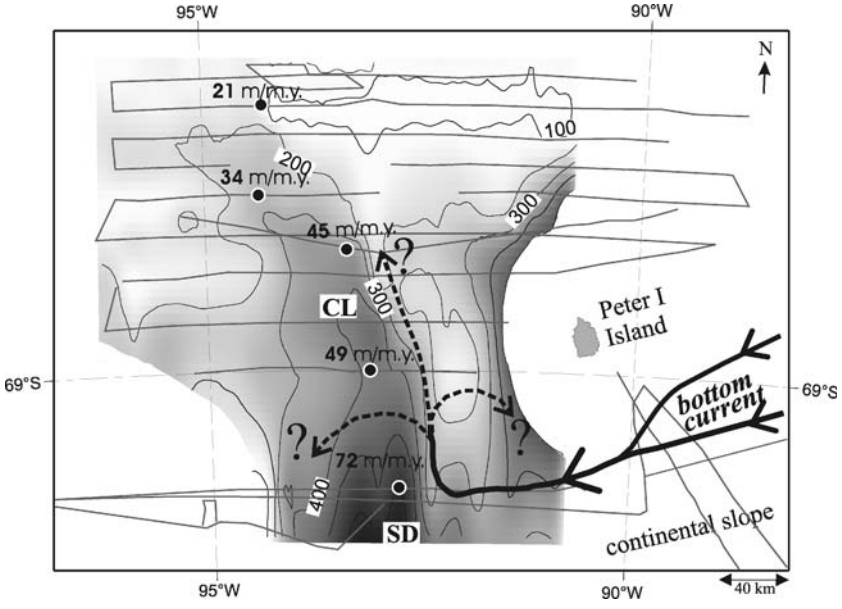

Fig. 11 Estimated sediment thickness of the youngest Cenozoic sediments, i.e. unit E1a of the sediment drift (*SD*) and the western channel levee (*CL*). The *isolines* show the thickness in meter. The base of this sediment body was estimated from the seismic profiles presented in this study (cf. base of channel levee, *LB*, on preceding figures). Five calculated maximum sediment accumulation rates are marked with *black/white points* at the respective locations (m/m.y. denotes metres per million years). The *arrows* display the estimated direction of the westward-flowing bottom current along the continental margin between Peter I Island up to the sediment drift (*SD*). Further continuation of the current remains uncertain (*dashed arrows*)

Sediment thicknesses and accumulation rates

As illustrated in Fig. 11, thicknesses vary between 600 m (BAS-92324) and less then 100 m (PET-98409) in the study area. The thickest segment of the levee on profile ANT-95201 at CDP 800 (about 0.22 s TWT, Fig. 6) is approx. 360 m thick. The generation of a time scale for individual sediment layers, required for the estimation of accumulation rates, is difficult in the present case due to the lack of drill data for this area. Correlations of sedimentary units of the study area with the nearest ODP sites (1095 and 1096 of Leg 178) are rather poor, as shown in the western part of seismic profile AWI-20010001 in Scheuer et al. (2006). Accretionary wedges, formed during Late Cretaceous to early Tertiary subduction along the continental margin, have been interpreted from the Continental Slope Gravity Anomaly (Cunningham et al. 2002). These wedges may have acted as a barrier against the downslope transport of sediments, leading to different forms of sediment accumulation on the continental rise of the Bellingshausen Sea (Scheuer et al. 2006). Site 324 of DSDP Leg 35, located west of the BGA, penetrated to a depth of only 218 m in Pleistocene and Pliocene sediments of mainly unconsolidated clay (Hollister and Craddock 1976) and, therefore, did not reach the sediments deposited at the base of the levee. However, for calculations of sediment accumulation rates, we can make assumptions about the onset of channel-levee development. It is likely that the channel-levee system developed with the onset of strong glacial sediment supply to the continental rise caused by regularly advancing grounding ice on the continental shelf (e.g. Rebesco et al. 1997). High sediment accumulation rates on the continental slope may have resulted in a more frequent occurrence of turbidites and, thus, the deposition of turbiditic sediments along the margins of erosional channels. The oldest drilled glacial sediment sequences on the western Antarctic Peninsula shelf were dated at about 9.6 Ma (e.g. Iwai et al. 2002; Barker and Camerlenghi 2002). We use this age for the calculation of accumulation rates along the SCS and MCS profiles selected for the present study.

Although such calculations of sediment accumulation rates do not account for the true width and volume of the levees, the data indicate a decline in sedimentation towards the north (Fig. 11). Sediment accumulation rate is highest along profile BAS-92324 (72 m/10^6 years) and strongly decreases northwards to 21 m/10^6 years along profile PET-98407 (Table 1).

The validity of these values can be assessed by a comparison with sediment accumulation rates for other depocentres of the West Antarctic continental margin. The highest value on the continental rise of the Antarctic Peninsula during the early Pliocene is about 180 m/10^6 years, calculated on the basis of magneto-biochronologic data from ODP site 1096 on Drift 7 (Iwai et al. 2002). The highest known accumulation rate along the West Antarctic continental margin since the Pliocene is about 295 m/10^6 years for a trough-mouth fan east of Peter I Island, referred to as Depocentre B and located approx. 150 km east of Depocentre C (Scheuer et al. 2006). This trough-mouth fan developed at the foot of a shelf trough and appears to be the main depocentre for terrigenous material eroded and transported by grounded ice on the shelf between Alexander and Thurston islands. This trough-mouth fan may be the origin for a large part of the early Cenozoic sediments deposited in the southern sector of Depocentre C, delivered by the westward-flowing bottom current (Ó Cofaigh et al. 2005; Scheuer et al. 2006). The maximum accumulation rate of 72 m/10^6 years for the southern sector of Depocentre C (cf. above) suggests a lower downslope input of sediments during the late Cenozoic, compared to these main depositional areas (Depocentre B and Drift 7).

Table 1 Maximum sediment thicknesses and accumulation rates of unit E1a along profile BAS-92324, and of the western levee along the other four profiles shown below (based on one common depth point, CDP, for each profile)

Profile	CDP/ trace	Compacted thickness TWT (s)	Compacted thickness (m)	Accumulation rate[a] (m/10^6 years)
BAS-92324	4,900	0.80	680	72
PET-98407	1,050	0.55	468	49
ANT-95201	1,000	0.50	425	45
PET-9840-3b	750	0.38	323	34
PET-98408	2,650	0.24	204	21

[a]Age of levee basis is ~9.6 Ma. The seismic interval velocity used for the calculation of sediment accumulation rate is 1,700 m/s, derived from the analysis of MCS profile AWI-95201 (cf. text for further information).

Due to the partially low quality of the seismic data used for the present study and to the lack of age control by ocean drilling, we are neither able to differentiate single turbiditic or contouritic sediment sequences, nor make inferences about glacial cycle influence on sediment supply in the western Bellingshausen Sea. Furthermore, indicators of palaeoceanographic conditions are, at present, too scarce to reconstruct bottom-current evolution during glacial and interglacial periods and, thus, any variability in bottom-current control of sediment accumulation. Nevertheless, the large size of Depocentre C and its unique setting in an uplifted region of oceanic basement earmark it as an important example of bottom-current influence on sediment accumulation along the Antarctic continental margin.

We assume that the structure of Depocentre C and sediment accumulations north of Peter I Island reflect the course of the westward-flowing bottom current (Fig. 11). The submarine foot of Peter I Island would act as topographic barrier. North of Peter I Island, sediment accumulations such as sediment drifts along the sides of seafloor depressions are not observed, arguing against

bottom-current activity in this region. The main part of the current probably flows between the continental slope and Peter I Island, causing the development of the sediment drift on profile BAS-92324. Similarly to recent bottom-current activity on Drift 7 (Rebesco et al. 2002), in the western Bellingshausen Sea the current may be diverted towards the north, following the topography as a contour current without provoking the continuation of the sediment drift to the north. Rather, the Coriolis force would be the decisive factor controlling sedimentation here. Nevertheless, the course of the current north of profile BAS-92324 remains unclear.

Acknowledgements We are grateful to the captain and crew of the RV *Akademik Boris Petrov* for their support during Cruise no. 29. The cruise was funded by the Alfred Wegener Institute for Polar and Marine Research, Bremerhaven, the Vernadsky Institute of Geochemistry and Analytical Chemistry, Moscow, and the Russian Foundation for Fundamental Investigation (RFFI). We thank Dr. A.F. Beresnev, Dr. P.N. Efimov and Eng. V.N. Poberzhin of the Vernadsky Institute for the acquisition of seismic data. We also acknowledge the British Antarctic Survey, especially Dr. Rob Larter, who provided the seismic data of profile BAS-92324.

References

Anderson JB, Wellner JS, Lowe AL, Mosola AB, Shipp SS (2001) The footprint of the expanded West Antarctic Ice Sheet: ice stream history and behaviour. GSA Today 11:4–9

Barker PF, Camerlenghi A (2002) Glacial history of the Antarctic Peninsula from Pacific margin sediments. In: Barker PF, Camerlenghi A, Acton GD, Ramsay ATS (eds) Proc ODP Sci Res 178. http://wwwodp.tamu.edu/publications/178_SR/synth/synth.htm

Bart PJ, Anderson JB (1995) Seismic record of glacial events affecting the Pacific margin of the northwestern Antarctic Peninsula. In: Cooper AK, Barker PF, Brancolini G (eds) Geology and seismic stratigraphy of the Antarctic margin. American Geophysical Union, Washington, District of Columbia, Antarctic Res Ser 68:75–95

Camerlenghi A, Crise A, Accerboni E, Laterza R, Pudsey CJ, Rebesco M (1997) Ten-month observation of the bottom current regime across a sediment drift on the Pacific of the Antarctic Peninsula. Antarctic Sci 9:424–431

Cooper AK, Barrett P, Hinz K, Traubea V, Leitchenkov G, Stagg H (1991) Cenozoic prograding sequences of the Antarctic continental margin: a record of glacioeustatic and tectonic events. Mar Geol 102:175–213

Cunningham AP, Larter RD, Barker PF (1994) Glacially prograded sequences on the Bellingshausen Sea continental margin near 90°W. Terra Antarctica 1:267–268

Cunningham AP, Larter RD, Barker PF, Gohl K, Nitsche FO (2002) Tectonic evolution of the pacific margin of Antarctica. 2. Structure of Late Cretaceous—early Tertiary plate boundaries in the Bellingshausen Sea from seismic reflection and gravity data. J Geophy Res 107(B12):2346 DOI 10.1029/2002JB001897

Eagles G, Gohl K, Larter RD (2004) Life of the Bellingshausen plate. Geophys Res Lett 31 L07603 DOI 10.1029/2003GL019127

Faugères J-C, Stow DAV, Imbert P, Viana A (1999) Seismic features diagnostic of contourite drifts. Mar Geol 162:1–38

Gohl K, Nitsche, FO, Miller H (1997) Seismic and gravity data reveal Tertiary intraplate subduction in the Bellingshausen Sea, southeast Pacific. Geology 25:371–374

Hampton MA, Eittreim SL, Richmond BM (1987) Post-breakup sedimentation on the Wilkes Land Margin, Antarctica. In: Eittreim SL, Hampton MA (eds) The Antarctic continental margin. Geology and geophysics of offshore Wilkes Land. Circum-Pacific Council for Energy and Mineral Recourses, Earth Science Series 5A, pp 75–89

Hollister CD, Craddock C (1976) Introduction, principal results. Leg 35 Deep Sea Drilling Project. Initial Reports Deep Sea Drilling Project 35. US Government Printing Office, Washington, District of Columbia

Iwai M, Acton GD, Lazarus D, Ostermann LE, Williams T (2002) Magnetobiochronologic synthesis of ODP Leg 178 rise sediments from the Pacific sector of the Southern Ocean: sites 1095, 1096 and 1101. In: Barker PF, Camerlenghi A, Acton GD, Ramsay ATS (eds) Proc ODP Sci Res 178:1–40 (CD-Rom)

Kuvaas B, Kristoffersen Y, Guseva J, Leitchenkov G, Gandjukhin V, Kudryavtsev G (2004) Input of glaciomarine sediments along the East Antarctic continental margin: depositional processes on the Cosmonaut Sea continental slope and rise and a regional acoustic stratigraphic correlation from 40W to 80E. Mar Geophys Res 25(3/4):247–263

Larter RD, Cunningham AP (1993) The depositional pattern and distribution of glacial-interglacial sequences on the Antarctic Peninsula Pacific margin. Mar Geol 109:203–219

Larter RD, Cunningham AP, Barker PF, Gohl K, Nitsche FO (2002) Tectonic evolution of the pacific margin of Antarctica. 1. Late Cretaceous tectonic reconstructions. J Geophys Res 107 B12 2345 DOI 10.1029/2000JB000052

Lucchi RG, Rebesco M, Camerlenghi A, Busetti M, Tomadin L, Villa G, Perisco D, Morigi C, Bonci MC, Giorgetti G (2002) Mid-late Pleistocene glacimarine sedimentary processes of a high-latitude, deep-sea sediment drift (Antarctic Peninsula Pacific margin). Mar Geol 189:343–370

McGinnes JP, Hayes DE, Driscoll NW (1997) Sedimentary processes across the continental rise of the southern Antarctic Peninsula. Mar Geol 141:91–109

Nitsche FO, Gohl K, Vanneste K, Miller H (1997) Seismic expression of glacially deposited sequences in the Bellingshausen and Amundsen Seas, West Antarctica. In: Barker PF, Cooper AK (eds) Geology and seismic stratigraphy of the Antarctic Margin, vol 2. American Geophysical Union, Washington, District of Columbia, Antarctic Res Ser 71:95–108

Nitsche FO, Cunningham AP, Larter RD, Gohl K (2000) Geometry and development of glacial continental margin depositional systems in the Bellingshausen Sea. Mar Geol 162:277–302

Nowlin WD, Zenk W (1988) Westward bottom currents along the margin of the South Shetland Island Arc. Deep-Sea Res 35 (2):269–301

Ó Cofaigh C, Larter RD, Dowdeswell JA, Hillenbrand C-D, Pudsey CJ, Evans J, Morris P (2005) Flow of the West Antarctic Ice Sheet on the continental margin of the Bellingshausen Sea at the Last Glacial Maximum. J Geophys Res 110 DOI 10.1029/2005JB003619

Rebesco M, Stow D (2001) Seismic expression of contourites and related deposits. Mar Geophys Res Spec Issue 22(5/6):303–308

Rebesco M, Larter RD, Camerlenghi A, Barker PF (1996) Giant sediment drifts on the continental rise west of the Antarctic Peninsula. Geo-Mar Lett 16:65–75

Rebesco M, Larter RD, Barker PF, Camerlenghi A, Vanneste LE (1997) History of sedimentation on the continental rise west of the Antarctic Peninsula. In: Cooper AK, Barker PF (eds) Geology and seismic stratigraphy on the Antarctic Margin, vol 2. American Geophysical Union, Washington, District of Columbia, Antarctic Res Ser 71:29–49

Rebesco M, Pudsey CJ, Canals M, Camerlenghi A, Barker PF, Estrada F, Giorgetti A (2002) Sediment drifts and deep-sea channel systems, Antarctic Peninsula Pacific margin, mid-Miocene to present. In: Stow DAV, Pudsey CJ, Howe J, Faugères J-C, Viana A (eds) Deep-water contourite systems: modern drifts and ancient series, seismic and sedimentary characteristics. Spec Publ Geol Soc Lond Mem 22:353–371

Scheuer C, Gohl K, Larter RD, Rebesco M, Udintsev G (2006) Variability in Cenozoic sedimentation along the continental rise of the Bellingshausen Sea, West Antarctica. Mar Geol 227:279–298

Smith WHF, Sandwell DT (1997) Global seafloor topography from satellite altimetry and ship depth soundings. Science 277: 1956–1961

Tomlinson JS, Pudsey CJ, Livermore RA, Larter RD, Barker PF (1992) Long-range sidescan sonar (GLORIA) survey of the Antarctic Peninsula Pacific margin. In: Yoshida Y, Kaminuma K, Shiraishi K (eds) Recent progress in Antarctic earth science. Terra, Tokyo, pp 423–429

Tucholke BE, Houtz RE (1976) Sedimentary framework of the Bellingshausen Basin from seismic profile data. In: Hollister CD, Craddock CD et al. (eds) Initial Reports Deep Sea Drilling Project 35. US Government Printing Office, Washington, District of Columbia, pp 197–227

Udintsev GB, Schenke GW, Schöne T, Beresnev AF, Efimov PN, Kol'tsova AV, Knyazev AB, Tererin DE, Kurentsova NA, Bulychev AA, Gilod DA (1999) New data on the floor structure of the Bellingshausen Sea, Western Antarctica. Dokl Earth Sci 367A(6):876–880